IEEE Access
Multidisciplinary | Rapid Review | Open Access Journal

Received July 2, 2018, accepted August 7, 2018, date of publication August 10, 2018, date of current version September 5, 2018.

*Digital Object Identifier 10.1109/ACCESS.2018.2864600*

# An Aerodynamics-Based Novel Optimal Power Extraction Strategy for Offshore Wind Farms With Central VSCs

**SI-ZHE CHEN[1], GUOZHUAN XIONG[1], GUIDONG ZHANG[1], (Member, IEEE), SAMSON SHENGLONG YU[2], (Student Member, IEEE), HERBERT HO-CHING IU[2], (Senior Member, IEEE), TYRONE FERNANDO[2], (Senior Member, IEEE), AND YUN ZHANG[1]**

[1]School of Automation, Guangdong University of Technology, Guangzhou 510006, China
[2]School of Electrical, Electronics, and Computer Engineering, The University of Western Australia, Perth, WA 6009, Australia

Corresponding author: Guidong Zhang (guidong.zhang@gdut.edu.cn)

This work was supported in part by the National Natural Science Foundation of China under Grant 51307025 and Grant U1501251, in part by the Science and Technology Planning Project of Guangdong Province under Grant 2017B090907011, in part by the Natural Science Foundation of Guangdong Province under Grant 2017A030310243, in part by the Foundation for Distinguished Young Talents in Higher Education of Guangdong under Grant 2016KQNCX039, and in part by the Australian Research Council Discovery Project under Grant DP170104426.

**ABSTRACT** Costly distributed converters are used in traditional offshore wind turbine generators (WTGs); recently, centralized voltage source converters (CVSC) have been utilized to replace the distributed ones for cost reduction. This method, however, reduces the wind energy that can be harvested from the environment, since all WTGs' synchronous rotational speeds depend on the frequency of the same CVSC but their wind speeds are generally different. To solve this problem, in this paper, a novel power optimization model is developed based on the aerodynamic characteristics of the wind in contact with the turbines. It is followed with the proposal of a novel maximum power generation strategy, using the particle swarm optimization algorithm. The proposed optimal power extraction (OPE) strategy can achieve the maximum power generation, and at the same time limit the excess power output to enhance operational safety. Simulation studies are conducted in this paper to validate the proposed OPE strategy for WTGs, which demonstrate the superiority of the proposed OPE strategy in harnessing the maximum energy from wind, in comparison to the existing method.

**INDEX TERMS** Centralized voltage source converters, optimal power extraction, particle swarm optimization, wind energy.

## I. INTRODUCTION

Recently, offshore wind energy has attracted substantial attention because of its techno-economic and environmental benefits, such as high energy intensity, steady power output, and no land occupation [1], [2]. Offshore wind farms need high voltage direct current (HVDC) or high voltage alternating current (HVAC) transmission to interface with the power grid [3], [4]. The HVDC transmission is widely used in long-distance transmission due to its unique advantages, i.e., lower losses, no limitations in length,and the ability to connect with much weaker networks [5], [6]. However, the applicability of HVDC for offshore wind farms is still restricted, due to its high costs associated with HVDC converters [7]–[9].

The first subfigure of FIGURE 1 shows a conventional offshore wind farm topology employing the HVDC transmission. Therein, WTGs connect to the AC bus through a set of distributed converters; the AC bus connects to the HVDC link through a VSC at the wind farm side. This setup is firstly non-economical due to the large number of power electronics devices required, and will also incur a significant amount of power losses during the power transmission. To replace the distributed converters, Jovcic and Strachan [10] proposed an offshore wind farm topology with centralized power conversion and multi-terminal HVDC connection, as shown in the second subfigure of FIGURE 1. In this structure, each VSC in the multi-terminal HVDC transmission provides

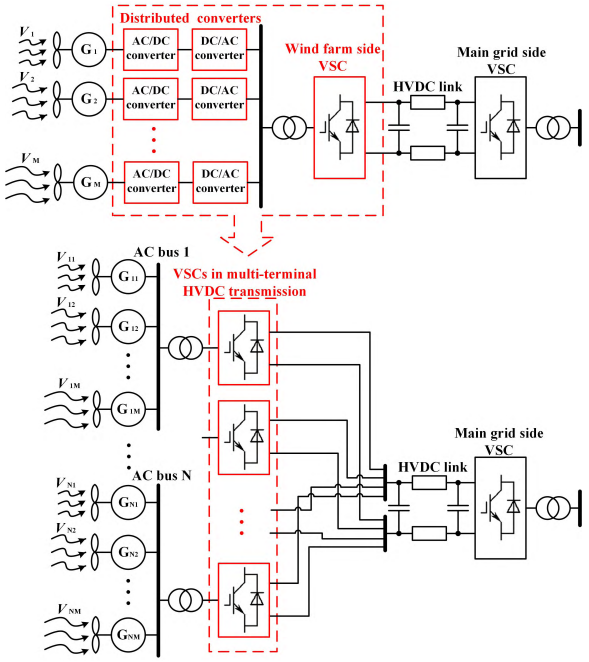


**FIGURE 1.** Comparison of conventional and centralized offshore wind farm topology [10].

variable speed control for a group of WTGs. It is noteworthy that all WTGs' synchronous rotational speeds are regulated by the same CVSC structure and control signals, but their wind speeds are generally different. Hence, WTGs could not all operate at the maximum power point, and therefore the overall wind power system fails to harness the maximum kinetic energy from the ambient environment. Compared to using distributed converters to interface wind turbines with the main grid, the traditional CVSC may lose some of the energy extracted from the wind. However, due to the centralized converter topology and the fact that most wind turbines in the same wind power plant received wind of similar velocity, CVSC is a valid option of integrating wind turbines into the main grid. Also, the maintenance cost is substantially lower for CVSC than distributed layouts. This has been well studied in [10]. This paper is actually trying to solve this issue and proposing a novel optimization method to enhance the energy extraction of centrally connected VSCs. The proposed optimal power extraction (OPE) strategy for CVSC-WTs can effectively improve the energy extraction efficiency of the traditional CVSCs-WTs.

To improve the overall performance of the WTGs, the group size was optimized based on the centralized topology by making a trade-off between power loss and costs [10]. Vrionis *et al.* [11] proposed a methodology to optimize the AC frequency for searching the optimal speed, which, however, may not be able to find the global optimum due to the highly non-convex optimization problem formed to reach the objective. Gomis-Bellmunt [12] proposed that wind energy efficiencies could be written as polynomials of tip speed ratios, in which all the pitch angles were set zero, and the Newton iteration method was adopted to compute the optimal frequency of the AC bus corresponding to maximum power generation. However, they both only consider how to find an optimal AC frequency, but harvesting the maximum power generation by a wind farm considering each turbine's distinct characteristics has not yet been fully addressed in the literature.

Existing work for optimal power extraction of WTGs is mainly considering one variable, i.e., the angular speed of WTGs or AC frequency, and only considering this factor cannot make the WTGs reach the best wind energy utilization. Another important factor, pitch angle, has not been incorporated in any of the existing work. In order to address this, a wind turbine model considering the aerodynamic characteristics is developed in this paper, and an optimal power extraction strategy is proposed thereafter for CVSC-connected offshore wind farms. The main novelty of the proposed OPE is that it preserves the advantages of the centralized VSC-connected WTGs, and it maximizes the kinetic energy that can be harnessed from the ambient wind by optimally controlling the operation statuses of the WTGs. Simulations show the superiority of the proposed OPE method in harnessing the maximum energy from wind, in comparison to the existing best method proposed in [12]. The OPE strategy is also easy to implement and does not entail any extra costly hardware, which also poses the economic advantage of this method.

The remainder of this paper is organized as follows. Section II describes the aerodynamic characteristics of the wind farm system, and a novel power optimization model is developed thereafter. An OPE strategy based on PSO algorithm is designed in Section III. Simulations are conducted to validate the effectiveness of proposed strategy in Section IV. Finally, this paper concludes in Section V.

## II. POWER OPTIMIZATION MODEL

### A. AERODYNAMIC CHARACTERISTIC ANALYSIS

According to *Bates theory* [13], the output power of a WTG is given as

$$P = \frac{1}{2} C_{\mathrm{p}}(\lambda, \beta) \rho A V^3, \tag{1}$$

where $\rho$ is the air density,$A$ is the area covered by the rotating blade of wind turbine, $V$ is the wind speed, while the wind energy efficiency $C_{\mathrm{p}}$ is

$$C_{\mathrm{p}}(\lambda, \beta) = c_1 \left(\frac{c_2}{\lambda_i} - c_3\beta - c_4\right) e^{\frac{-c_5}{\lambda_i}} + c_6\lambda, \tag{2}$$

where $\lambda$ is the tip speed ratio; $\beta$ is the pitch angle of blade; $c_1$ to $c_6$ are constant coefficients and given in TABLE 1; and one has the expression of $\lambda_i$ as

$$\frac{1}{\lambda_i} = \frac{1}{\lambda + 0.08\beta} - \frac{0.035}{\beta^3 + 1}. \tag{3}$$

The tip speed ratio $\lambda$ reads

$$\lambda = \frac{\omega_{\mathrm{t}} R}{V} = \frac{\omega_{\mathrm{g}} R}{n_{\mathrm{g}} V}, \tag{4}$$

where $\omega_t$ and $\omega_g$ are the angular speeds of wind turbine and generator, respectively; $R$ is the length of blades; while $n_g$ is the ratio of gearbox.

According to (2) and (3), the wind energy efficiency $C_p$ with different tip speed ratios and pitch angles are depicted in FIGURE 2.

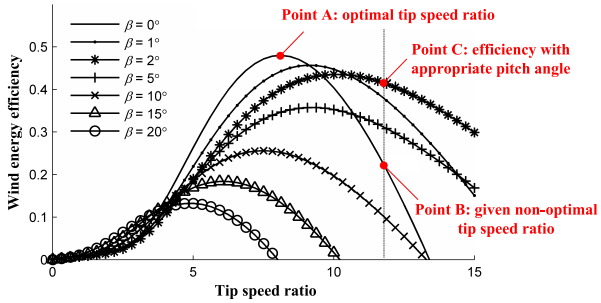


**FIGURE 2. Wind energy efficiency with different tip speed ratios and pitch angles.**

All WTGs' synchronous rotation speeds depend on the frequency of a same CVSC. However, due to some influences such as wake effect, the wind speeds of WTGs are all different. Hence, the WTGs can't all operate at the optimal tip speed ratio, which results in the whole system unable to reach the highest energy efficiency.

Since WTGs with high wind speed have more generating potential, they should operate at a point close to optimal tip speed ratio, as the point A of FIGURE 2, which ensures their wind energy efficiency. In this case, since all WTGs' synchronous rotation speeds are the same, for WTGs with low wind speed, their tip speed ratios are inevitably deviated from the optimal value, which will reduce the wind energy efficiency, as the point B of FIGURE 2. According to FIGURE 2, the wind energy efficiency of WTGs operating at given non-optimal tip speed ratio can be significantly improved by selecting an appropriate pitch angle,as the point C.

Hence, the maximum power generation control for a group of WTGs with centralized power conversion is a multi-variable optimization problem, in which the total generation power depends on the unified angular speed and all the individual pitch angles of each WTG.

### B. POWER OPTIMIZATION MODEL DEVELOPMENT

The target of power optimization is to seek the optimal angular speed and pitch angles corresponding to the maximum power from a group of WTGs which is given as

$$P_{\text{sum}} = \sum_{j=1}^{M} P_j, \tag{5}$$

where $P_j$ is the output power of the $j$-th WTG, and $M$ is the number of WTGs in a group.

To display the angular speed of WTG in the target function, (3) and (4) are substituted into (2), and the wind energy efficiency is rewritten as follows,

$$C_p(V,\beta,\omega_g) = c_1\left(\frac{c_2}{\frac{\omega_g R}{ngV}+0.08\beta} - \frac{0.035c_2}{\beta^3+1} - c_3\beta - c_4\right) \times e^{\frac{-c_5}{\frac{\omega_g R}{ngV}+0.08\beta}+\frac{0.035c_5}{\beta^3+1}} + c_6\frac{\omega_g R}{ngV}. \tag{6}$$

According to (1) and (6), (5) can be rewritten as

$$P_{\text{sum}} = \frac{1}{2}\rho A\sum_{j=1}^{M} C_p(V_j,\beta_j,\omega_g)V_j^3. \tag{7}$$

According to the limitations of the adjustment ranges, the constraints of angular speed and pitch angles are given as

$$0 \le \omega_g \le \omega_{\text{rated}}, \tag{8}$$

and

$$\beta_{\min} \le \beta_j \le \beta_{\max}, \tag{9}$$

where $\beta_j$ is the pitch angle of the $j$-th WTG.

To ensure safe operations, the output powers of each WTG cannot exceed the rated power [14], and the constraint of output power is thus given as

$$P_j \le P_{\text{rated}}. \tag{10}$$

Since $P_j$ is not a variable in (7), the limitation of output power could not be treated the same way as angular speed and pitch angles. A penalty function to avoid overpower is thus introduced as

$$PEN_j = \begin{cases} P_j - P_{\text{rated}}, & P_j > P_{\text{rated}}, \\ 0, & P_j \le P_{\text{rated}}. \end{cases} \tag{11}$$

Combining (7) and the penalty function (11), the target function with the ability to limit output power of each WTG is given as

$$\max: F = \frac{1}{2}\rho A\sum_{j=1}^{M} C_p(V_j,\beta_j,\omega_g)V_j^3 - b\sum_{j=1}^{M} PEN_j, \tag{12}$$

where $b$ is penalty factor for overpower.

According to (11), when the output power of any WTG exceeds its rated power, the fitness of target function (12) will decrease. If the penalty factor $b$ is large enough, in the process of searching the maximum fitness value of the target function (12), the optimization algorithm will automatically avoid overpower.

## III. THE PROPOSED OPE STRATEGY

### A. MAXIMUM POWER GENERATION STRATEGY BASED ON PSO ALGORITHM

The PSO algorithm is an optimization method that can be applied into multi-variable functions with many local optimal points [15]. Its advantages include easy implementation, fast convergence, and good robustness [16]. Hence, PSO algorithm has been widely applied to maximum power point tracking (MPPT) of photovoltaic systems [17], [18], cooperative planning of active distribution system with renewable

energy sources and energy storage systems [19], design of wind farm configuration [20], and distributed optimal reactive power control of power systems [21].

According to the power optimization model developed in Section II, a novel OPE strategy for wind farms connected to central VSCs is proposed using the PSO algorithm. Steps of the proposed algorithm are given as follows with the flowchart shown in FIGURE 3, which are adopted and modified based on [18].

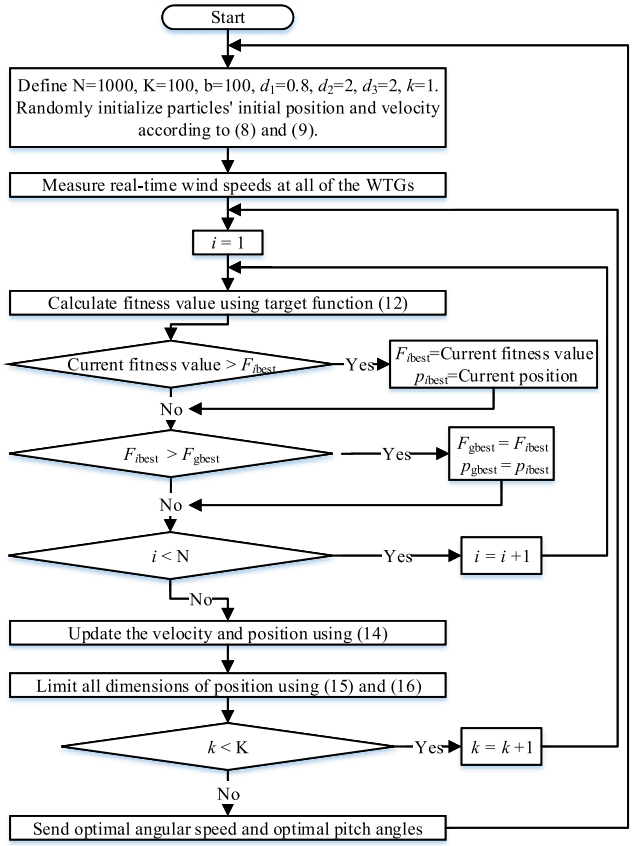


**FIGURE 3.** Flowchart of the proposed OPE strategy.

1) Parameter selection: For the proposed OPE strategy, the unified angular speed $\omega_g$ and all the pitch angles $\beta_j$ ($j$=1,2,...,$M$) of each WTG is defined as the particle position shown as (13), and the target function (12) is chosen as the fitness value evaluation function.

$$x = [w_g, \beta_1, \beta_2, \ldots, \beta_M]^T. \tag{13}$$

2) PSO Initialization: Input particle swarm size $N$, number of iterations $K$, penalty factor $b$, weight coefficients $d_1$, $d_2$, and $d_3$. Initial position and velocity of each particle are randomly initialized in the range defined as (8) and (9). Denote the initial iterative algebra as $k$=1.

3) Fitness evaluation: The fitness evaluation of each particle $i$ ($i = 1, 2, \ldots,$N) will be conducted using (12) according to its position represented as (13) and all of the WTGs' measured real-time wind speeds.

4) Determination of individual and global best fitness: New calculated fitness value of each particle $i$ ($i$=1,2,...,$N$) is compared with its previous individual best fitness value $F_{ibest}$, and the bigger fitness value and corresponding position will be recorded as the new individual best fitness value $F_{ibest}$ and individual best position $p_{ibest}$, respectively. And then, the new individual best fitness value $F_{ibest}$ are compared with previous global best fitness value $F_{gbest}$, and the bigger fitness value and corresponding position will be recorded as the new global best fitness value $F_{gbest}$ and global best position $p_{gbest}$, respectively.

5) Updating the velocity and position of each particle: The velocity and position of each particle in the swarm are updated in terms of

$$\begin{cases} v_i^{k+1} = d_1 v_i^k + d_2 r_1 (P_{ibest} - x_i^k) + d_3 r_2 (P_{gbest} - x_i^k), \\ x_i^{k+1} = x_i^k + v_i^{k+1}, \\ i = 1, 2, \ldots, N, \end{cases} \tag{14}$$

where $v_i$ and $x_i$ are the velocity and position of i-th particle, respectively; $d_1$, $d_2$, and $d_3$ are the weight coefficients; $r_1$ and $r_2$ are random numbers ranged in [0, 1]; $p_{ibest}$ is the individual best position of $i$-th particle; $p_{gbest}$ is the global best position; while superscript $k$ represents the iterative algebra.

6) Constraints judgment: If any dimensions of each particle's position exceed the constraints of angular speed and pitch angles given in (8) and (9), these dimensions should be replaced with the extreme values according to

$$\begin{cases} \beta_{i,j}^{k+1} = 0, & \beta_{i,j}^{k+1} \le 0, \\ \beta_{i,j}^{k+1} = \beta_{i,j}^{k+1}, & 0 \le \beta_{i,j}^{k+1} \le \beta_{\max}, \\ \beta_{i,j}^{k+1} = \beta_{\max}, & \beta_{i,j}^{k+1} > \beta_{\max}, \\ i = 1, 2, \ldots, N, & j = 1, 2, \ldots, M. \end{cases} \tag{15}$$

$$\begin{cases} \omega_{gi}^{k+1} = 0, & \omega_{gi}^{k+1} \le 0, \\ \omega_{gi}^{k+1} = \omega_{gi}^{k+1}, & 0 \le \omega_{gi}^{k+1} \le \omega_{\max}, \\ \omega_{gi}^{k+1} = \omega_{rated}, & \omega_{i,j}^{gi} > \omega_{rated}, \\ i = 1, 2, \ldots, N. \end{cases} \tag{16}$$

7) Stopping criterion: If the iterative algebra $k$ is smaller than the predefined number of iterations $K$, set $k = k + 1$ and go to step 3. If $k$ is equal to $K$, the end criterion is met, and the current global best position is output and given as

$$p_{gbest} = [\omega_{gbest}, \beta_{1best}, \beta_{2best}, \ldots, \beta_{Mbest}]^T, \tag{17}$$

where $\omega_{gbest}$ is the optimal angular speed, and $\beta_{jbest}$ is the optimal pitch angle of the $j$-th WTG.

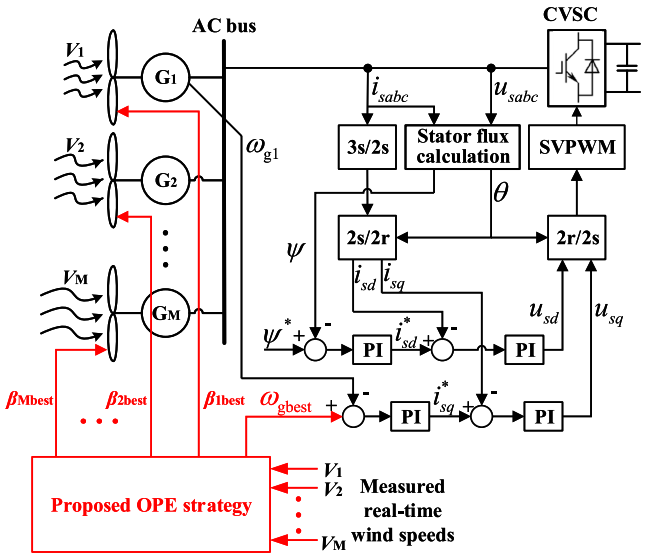


**FIGURE 4.** Block diagram of the control scheme using the proposed OPE strategy.

### B. CONTROL SCHEME OF THE VSC IN A MULTI-TERMINAL HVDC TRANSMISSION

FIGURE 4 shows the control scheme of a VSC in multi-terminal HVDC transmission. A flux-oriented vector controller is designed to control the flux and the angular speed of WTGs [10]. The amplitude $\psi$ and angle $\theta$ of the flux in FIGURE 4 are calculated according to the three phase voltages $u_{\text{sabc}}$ three phase currents $i_{\text{sabc}}$ measured from the AC bus, and then the direct-axis current $i_{\text{sd}}$ and quadrature-axis current $i_{\text{q}}$ in the flux-oriented synchronous reference frame are calculated. Since the synchronous rotation speeds of all WTGs in the same group depend on the frequency of the same VSC, the difference in the rotational speeds of the grouped generators are negligible. Therefore, in this study, the rotational speed of the first generator in the group is used to as the feedback signal to the angular speed controller.

In the control scheme, shown in FIGURE 4, the optimal angular speed $\omega_{\text{gbest}}$ computed by the proposed OPE strategy based on the PSO algorithm is adopted as the angular speed reference of the vector controller. The optimal pitch angles $\beta_{j\text{best}}$ computed by the proposed OPE strategy are adopted as the pitch angle reference of the $j$-th WTG, respectively.

## IV. CASE STUDY AND SIMULATION RESULTS

The simulation is performed in MATLAB/SIMULINK® 2010b on a desktop computer with Intel®Core i7-6700, 3.4GHz CPU and 64-bit Windows®7 operating system. In the simulation model, four WTGs based on squirrel-cage induction generator (SCIG) are connected to a single VSC, which is controlled by the proposed OPE control scheme given in FIGURE 4. The parameters of WTGs are shown in TABLE 1 and TABLE 2, and the parameters of PSO algorithm are shown in TABLE 3.

**TABLE 1.** Parameters of wind turbines.

| Parameter | Value |
|---|---|
| Rated power | 2.3 MW |
| Rated wind speed | 12 m/s |
| Length of blades | 37.96 m |
| Air density | 1.225 kg.m2 |
| Gearbox ratio | 61.35 |
| Maximum wind energy efficiency | 48 |
| Adjusting range of pitch angle | 0 - 90$^o$ |
| Wind turbine coefficient $c_1$ - $c_6$ | 0.5176, 116, 0.4, 5, 21, 0.0068 |

**TABLE 2.** Parameters of squirrel-cage induction generators.

| Parameter | Value |
|---|---|
| Rated line voltage | 690 V |
| Rated angular speed | 1500 RPM |
| Stator winding resistance | 1.102 mΩ |
| Rotor winding resistance (referred to the stator) | 1.497 mΩ |
| Magnetizing inductance (referred to the stator) | 2.13461 mH |
| Stator leakage inductance | 0.06492 mH |
| Rotor leakage inductance (referred to the stator) | 0.06492 mH |
| Moment of inertia | 1200Kg.m2 |
| Pole-pairs | 2 |

**TABLE 3.** Parameters of PSO algorithm.

| Parameter | Value |
|---|---|
| Weight coefficient $d_1$ | 0.8 |
| Weight coefficient $d_2$ | 2 |
| Weight coefficient $d_3$ | 2 |
| Penalty factor $b$ | 100 |
| Particle number $N$ | 1000 |
| Number of iterations $K$ | 100 |

### A. CASE 1: LOW TO MEDIUM WIND SPEEDS

The maximum power generation strategy proposed in [12] is also simulated using the same simulation model and conditions in this paper for comparison. The method in [12] only optimizes the frequency of the electricity at the AC bus, and it is called the "conventional optimization strategy" in this section.

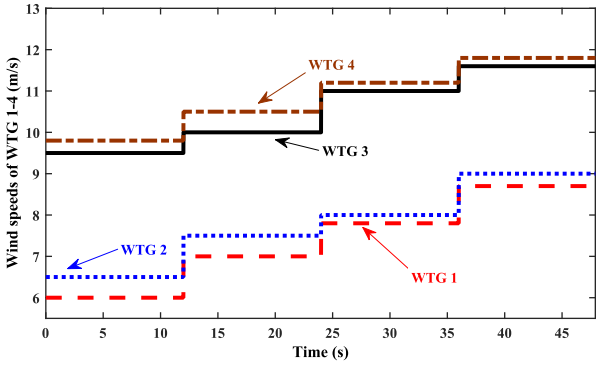


**FIGURE 5.** Wind speeds at each WTG in Case 1.

With wind speeds given in FIGURE 5, the optimization results of the PSO algorithm proposed in this paper and the conventional optimization algorithm proposed in [12] are given in FIGURE 6∼FIGURE 11.

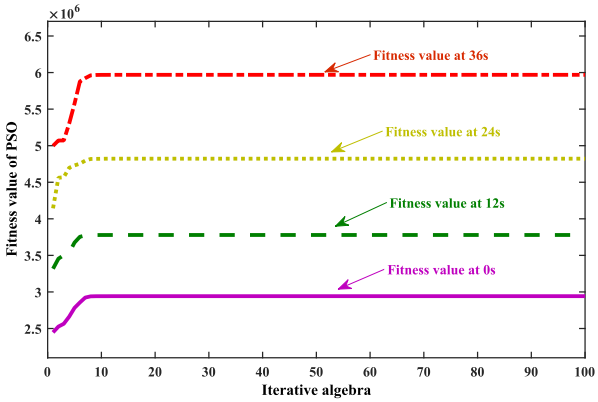


**FIGURE 6.** Fitness evaluation results of the PSO algorithm at each given time in Case 1.

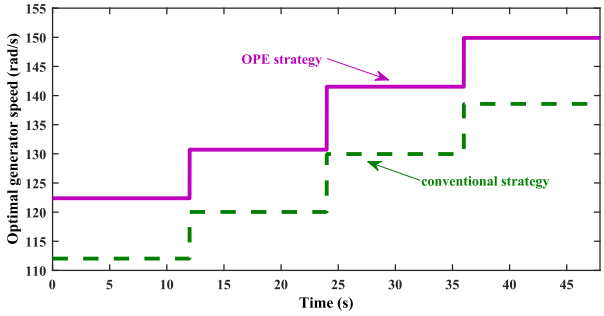


**FIGURE 7.** Comparison of optimal angular speeds in Case 1.

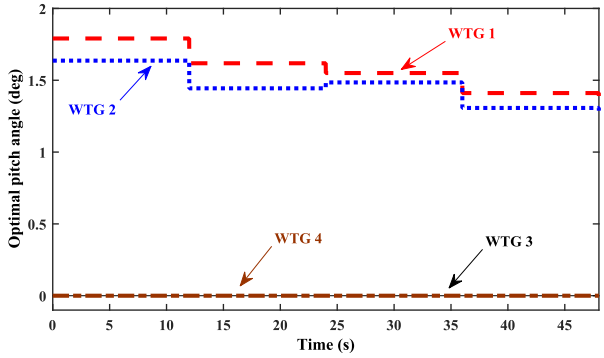


**FIGURE 8.** Optimal pitch angles of each WTG in Case 1.

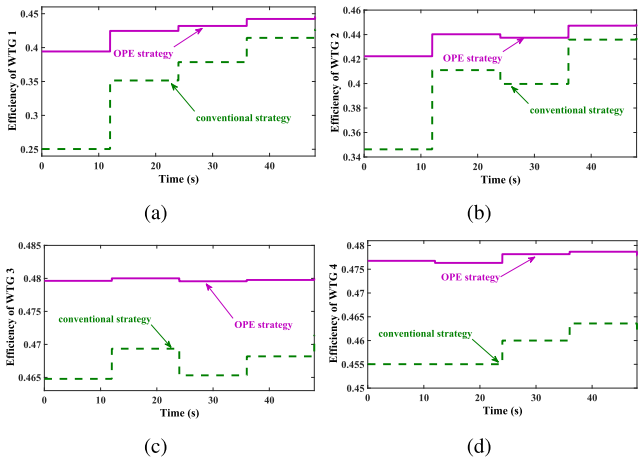


**FIGURE 9.** Comparison of wind energy efficiencies in Case 1: (a) Wind energy efficiency of WTG 1, (b) Wind energy efficiency of WTG 2, (c) Wind energy efficiency of WTG 3, and (d) Wind energy efficiency of WTG 4.

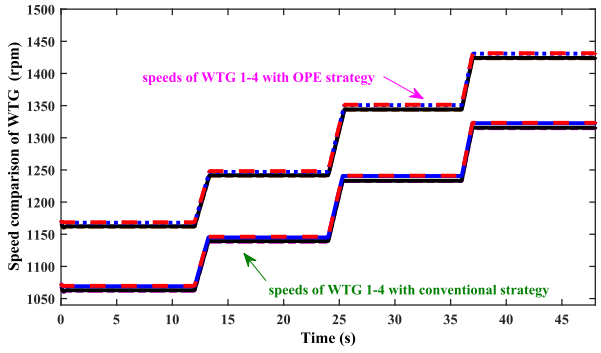


**FIGURE 10.** Individual rotating speed of each WTG in Case 1.

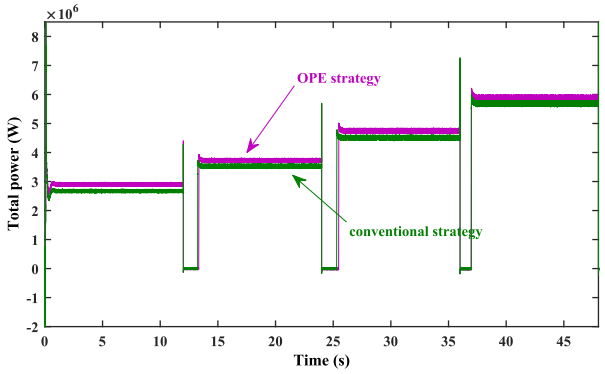


**FIGURE 11.** Total output power from all WTGs in Case 1.

The fitness evaluation results of the PSO algorithm at each given time are shown in. All the iterative calculations with different wind speeds quickly converge to the optimal fitness value, which shows a satisfactory real-time performance of the algorithm.

FIGURE 7 shows the optimal angular speeds computed by both algorithms, and FIGURE 8 shows the optimal pitch angles of each WTG computed by the proposed PSO algorithm, where all the pitch angles are zero in the conventional optimization algorithm. FIGURE 9 shows the wind energy efficiency of each WTG computed by both algorithms. Obviously, in FIGURE 7, the optimal angular speed computed by the proposed OPE algorithm is higher than the conventional method. In FIGURE 8, the optimal pitch angles of WTG 1 and WTG 2 (with low wind speed) are about 1.5, and the optimal pitch angles of WTG 3 and WTG 4 (with high wind speed) are about zero. In FIGURE 9, the wind energy efficiencies of each WTG computed by the proposed PSO algorithm are all higher compared with the conventional optimization algorithm. All the computation results shown in FIGURE 7∼FIGURE 9 have validated the OPE strategy

proposed in this paper, where WTGs with high wind speed operate at optimal tip speed ratio and the wind energy efficiency of WTGs with low wind speed can be improved by using appropriate pitch angles.

The individual rotating speeds of each WTG with both algorithms are shown in FIGURE 10, and the total output power from all WTGs are shown in FIGURE 11. It shows that the output power of the proposed OPE algorithm is higher than the output power of the conventional optimization algorithm.

In order to accelerate the WTGs to the optimal angular speed in shortest time as shown in FIGURE 10, the flux-oriented vector controller automatically reduces output power to zero as shown in FIGURE 11, and the harvested wind energy are totally used to accelerate the WTGs. If these power fluctuations cannot be accepted by the power grid, the changing rate of angular speed reference should be limited, which can reduce power fluctuations but extend the time of the dynamic process.

### B. CASE 2: MEDIUM TO HIGH WIND SPEEDS

It's known that the main control objective of pitch angle is to limit the output power of WTG when wind speed exceeds the rated value. To verify the effectiveness of power limitation of the proposed OPE algorithm, a new set of wind speeds for simulation are used, which are shown in FIGURE 12. The fitness evaluation results given in FIGURE 13 show that the iterative calculations can also converge to the optimal fitness value quickly.

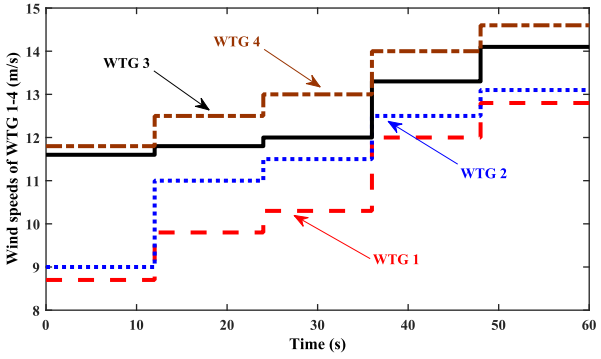


**FIGURE 12.** Wind speeds at each WTG in Case 2.

FIGURE 14∼FIGURE 16 show the optimal pitch angles, wind energy efficiency, and output power of each WTG, respectively.

During 0∼12s, all the wind speeds and output powers of each WTG are below the rated value. The pitch angles of the WTG 3 and WTG 4 (with high wind speed) are about zero, which makes them operate near maximum wind energy efficiency. The pitch angles of WTG 1 and WTG 2 (with low wind speed) are not zero, which maximize their wind energy efficiency at the given non-optimal rotating speed. This shows great congruity to the rationale behind the proposed OPE strategy as stated in Section II.

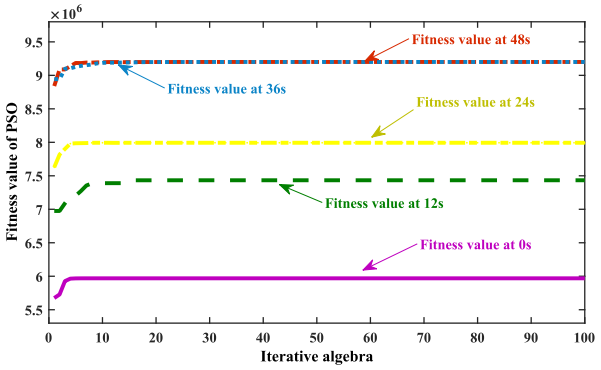


**FIGURE 13.** Fitness evaluation results of the PSO algorithm at each given time in Case 2.

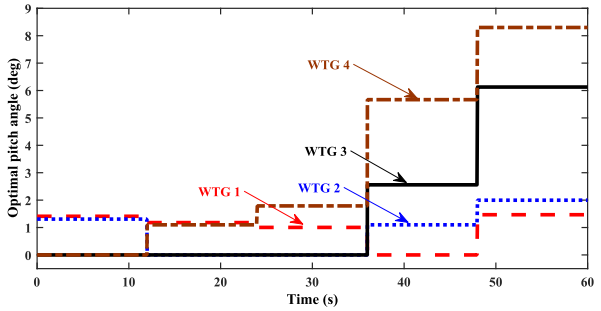


**FIGURE 14.** Optimal pitch angles of each WTG in Case 2.

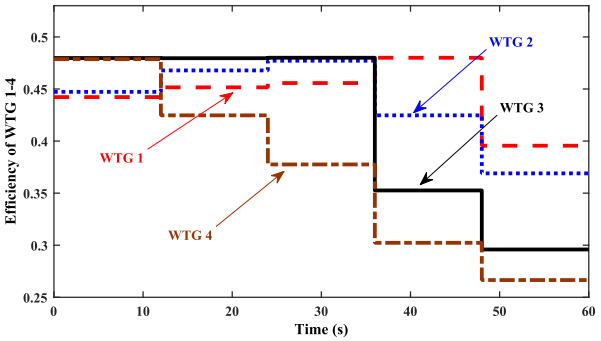


**FIGURE 15.** Wind energy efficiencies of each WTG in Case 2.

During 12∼36s, all the wind speeds increase, and the wind speed at WTG 4 exceeds the rated value. The pitch angles of WTG 2 and WTG 3 are about zero, and both of them operate at the maximum energy efficiency point. The pitch angle of WTG 1 decreases to maximize its wind energy efficiency at the non-optimal rotating speed. The pitch angle of WTG4 increase to limit its output power, and hence its wind energy efficiency decreases for safety reason. The simulation results during 12∼36s verify that the proposed OPE algorithm can limit the output power of WTG within the rated value if its wind speed exceeds the maximum allowable value, and at the same time maximize the output power of other WTGs.

During 36∼48s, the wind speed at the 1st WTG is below rated value, and hence its pitch angle is zero to make it operate

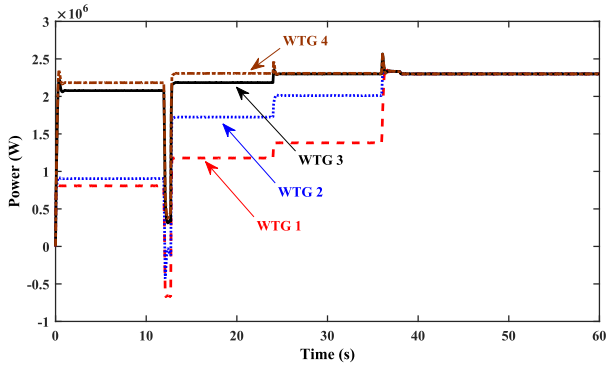


**FIGURE 16.** Output power of each WTG in Case 2.

near maximum wind energy efficiency. The pitch angles of the other WTGs increase to limit their output powers at the rated value. During 48∼60s, all the wind speeds exceed rated value, and hence all the pitch angles increase to limit the output powers of each WTG at rated value, respectively. The simulation results during 36∼60s verify that the proposed OPE algorithm can limit all the output power at rated value if all the WTGs are in contact with high wind speeds.

### C. CASE 3-5: VARIOUS WTG GROUP SIZES WITH REAL WIND SPEEDS

To analyze the proposed OPE algorithm under more practical conditions, we employ realistic wind speeds, which are shown in FIGURE 17 [22]. The WTG 8 is assumed as the first WTG in the direction of the wind with the highest wind speed, and wind speeds of other WTGs are gradually decreased by 0.5 m/s and delayed by 2 s, in order to simulate the influences of WTGs positions and wake effects [23].

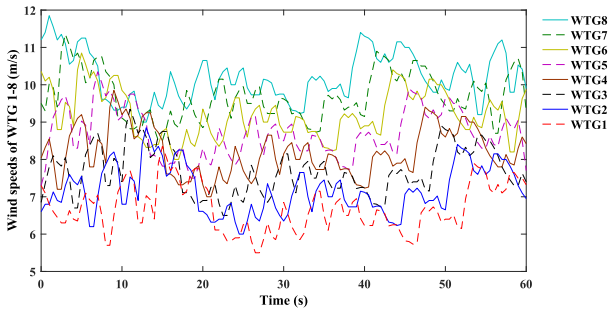


**FIGURE 17.** Wind speed at each WTG in Case 3-5.

In Case 3, four WTGs are grouped and controlled by a CVSC, including WTG 2, 4, 6, and 8. In Case 4, six WTGs are grouped and controlled by a CVSC, including WTG 1, 2, 4, 6, 7, and 8. In Case 5, all the eight WTGs are grouped and controlled by a CVSC.

FIGURE 18 shows the optimal generator speeds computed by the proposed OPE strategy and conventional optimization strategy [12]. FIGURE 19-21 shows the optimal pitch angles of each WTG computed by the proposed PSO algorithm

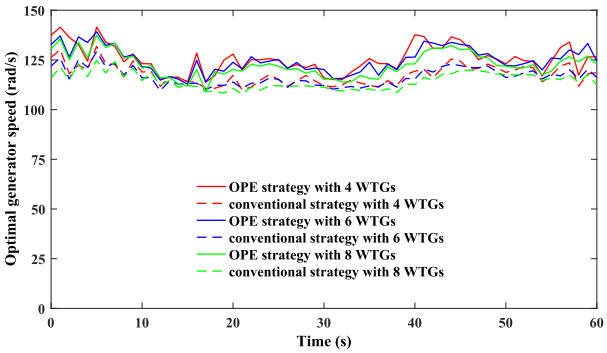


**FIGURE 18.** Comparison of optimal generator speeds in Case 3-5.

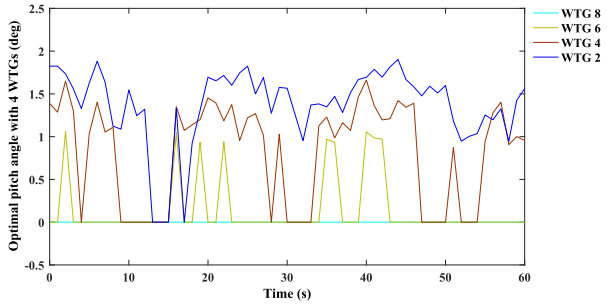


**FIGURE 19.** Optimal pitch angles of each WTG in Case 3.

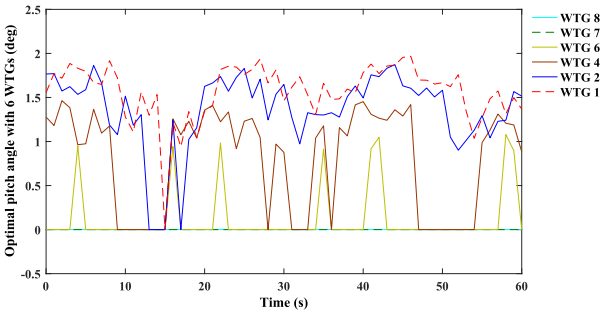


**FIGURE 20.** Optimal pitch angles of each WTG in Case 4.

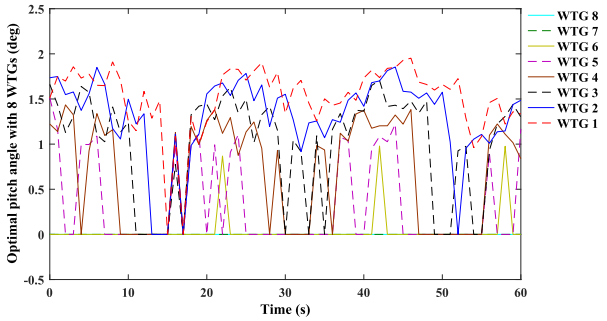


**FIGURE 21.** Optimal pitch angles of each WTG in Case 5.

in Case 3-5, respectively. FIGURE 22-24 shows the wind energy efficiency of each WTG computed by both algorithms in Case 3-5, respectively. Finally, FIGURE 25 shows the

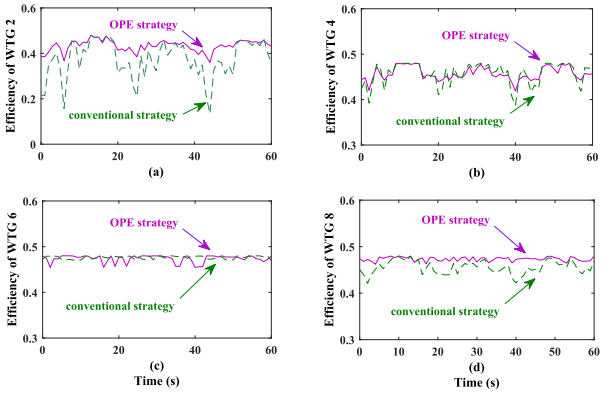


**FIGURE 22.** Comparison of wind energy efficiencies in Case 3: (a) Wind energy efficiency of WTG 2; (b) Wind energy efficiency of WTG 4; (c) Wind energy efficiency of WTG 6; and (d) Wind energy efficiency of WTG 8.

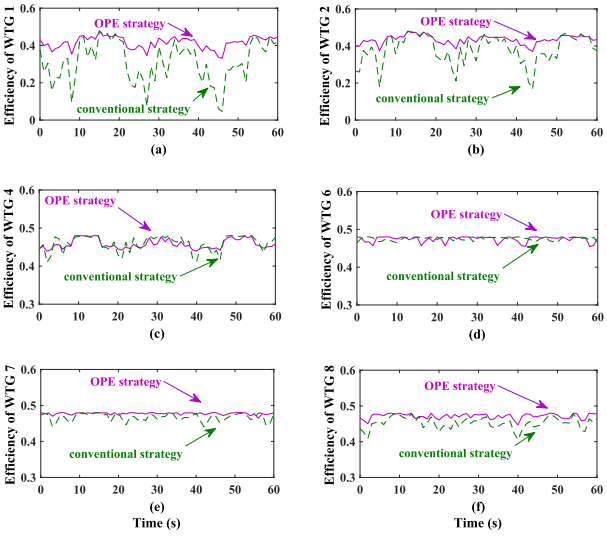


**FIGURE 23.** Comparison of wind energy efficiencies in Case 4: (a) Wind energy efficiency of WTG 1; (b) Wind energy efficiency of WTG 2; (c) Wind energy efficiency of WTG 4; (d) Wind energy efficiency of WTG 6; (e) Wind energy efficiency of WTG 7; and (f) Wind energy efficiency of WTG 8.

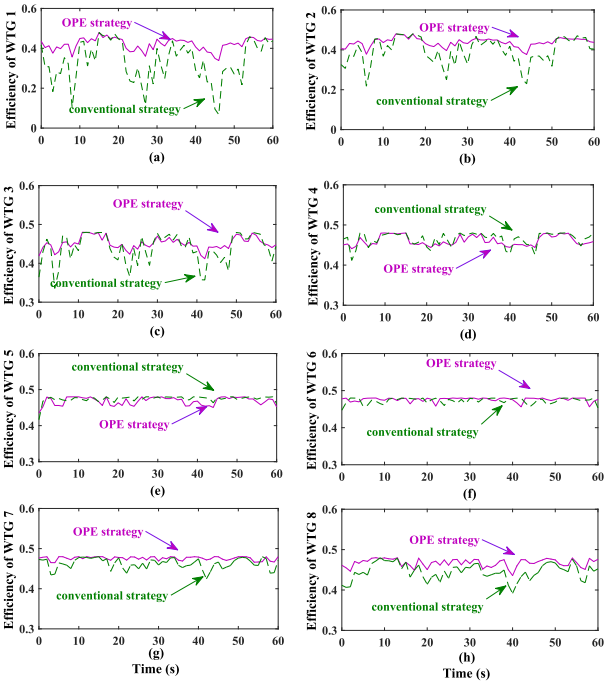


**FIGURE 24.** Comparison of wind energy efficiencies in Case 5: (a) Wind energy efficiency of WTG 1; (b) Wind energy efficiency of WTG 2; (c) Wind energy efficiency of WTG 3; (d) Wind energy efficiency of WTG 4; (e) Wind energy efficiency of WTG 5; (f) Wind energy efficiency of WTG 6; (g) Wind energy efficiency of WTG 7; and (h) Wind energy efficiency of WTG 8.

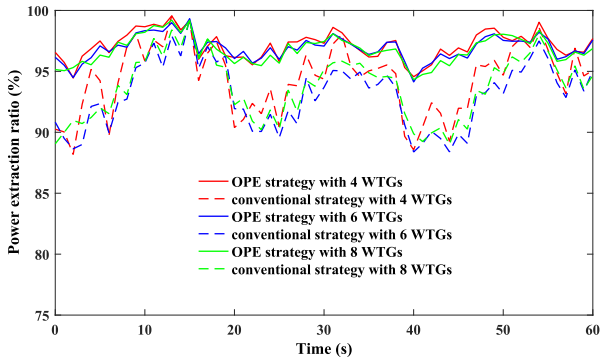


**FIGURE 25.** Comparison of power extraction ratio in Case 3-5.

ratios of extraction powers relative to the maximum available power obtained by using distributed converters for each wind turbine.

In FIGURE 18, the optimal generator speed of the proposed OPE algorithm is higher than the corresponding conventional method in each case. In FIGURE 19-21, it can be seen that the WTGs with relatively lower wind speeds operate at relatively larger pitch angles in each Case.

In FIGURE 22-24, the proposed OPE algorithm significantly improve the wind energy efficiencies of the WTGs with high wind speeds, such as WTG 8 in Case 3, WTG 7 and 8 in Case 4, and WTG 7 and 8 in Case 5. The reason is that the proposed OPE algorithm makes the WTGs with greater generating potential operate closer to the optimal tip speed ratio. In FIGURE 22-24, the proposed OPE algorithm also significantly improves the wind energy efficiencies of the WTGs with low wind speeds, such as WTG 2 in Case 3, WTG 1 and 2 in Case 4, and WTG 1, 2, and 3 in Case 5. The reason is that the wind energy efficiencies of WTGs operating at large tip speed ratios can be significantly improved by selecting appropriate pitch angles, as shown in FIGURE 2. However, the proposed OPE algorithm slightly decreases the wind energy efficiencies of WTGs with mid wind speeds, such as WTG 4 and 6 in Case 3, WTG 4 and 6 in Case 4, and WTG 4, 5, and 6 in Case 5.

As shown in FIGURE 25, compared with the conventional strategy, the proposed OPE algorithm improves the total power extraction ratio in each case, and the average wind energy losses caused by centralized power conversion are reduced to 3-3.5%.

## V. CONCLUSIONS

This paper proposes a novel optimal power extraction method for WTGs connected to central VSCs, which are fed to HVDC transmission lines. The proposed OPE strategy considers the aerodynamic characteristics to maximize the total output power by seeking the optimal angular speeds and pitch angles of each WTG. Simulation results have demonstrated that compared to the existing offshore WTG control methods, the proposed OPE strategy is able to optimally increase the total amount of power generated by WTGs connected to central VSCs, and simultaneously prevent the output power of each WTG from exceeding rated power, hence improving safety.

## REFERENCES

[1] T. A. T. Nguyen and S.-Y. Chou, "Maintenance strategy selection for improving cost-effectiveness of offshore wind systems," *Energy Convers. Manage.*, vol. 157, pp. 86–95, Feb. 2018.
[2] H. Chen, T. Tang, N. Aït-Ahmed, M. El Hachemi Benbouzid, M. Machmoum, and M. El-Hadi Zaïm, "Attraction, challenge and current status of marine current energy," *IEEE Access*, vol. 6, pp. 12665–12685, 2018.
[3] C. MacIver, K. R. W. Bell, and D. P. Nedić, "A reliability evaluation of offshore HVDC grid configuration options," *IEEE Trans. Power Del.*, vol. 31, no. 2, pp. 810–819, Apr. 2016.
[4] A. Raza *et al.*, "Power dispatch and voltage control in multiterminal HVDC systems: A flexible approach," *IEEE Access*, vol. 5, pp. 24608–24616, 2017.
[5] Y. Pipelzadeh, N. R. Chaudhuri, B. Chaudhuri, and T. C. Green, "Coordinated control of offshore wind farm and onshore HVDC converter for effective power oscillation damping," *IEEE Trans. Power Syst.*, vol. 32, no. 3, pp. 1860–1872, May 2017.
[6] H. Dong, Z. Xu, P. Song, G. Tang, Q. Xu, and L. Sun, "Optimized power redistribution of offshore wind farms integrated VSC-MTDC transmissions after onshore converter outage," *IEEE Trans. Ind. Electron.*, vol. 64, no. 11, pp. 8948–8958, Nov. 2017.
[7] S. Lauria, M. Schembari, F. Palone, and M. Maccioni, "Very long distance connection of gigawatt-size offshore wind farms: Extra high-voltage AC versus high-voltage DC cost comparison," *IET Renew. Power Gener.*, vol. 10, no. 5, pp. 713–720, May 2016.
[8] M. A. Parker and O. Anaya-Lara, "Cost and losses associated with offshore wind farm collection networks which centralise the turbine power electronic converters," *IET Renew. Power Gener.*, vol. 7, no. 4, pp. 390–400, Jul. 2013.
[9] G. Zhang, Z. Li, B. Zhang, and W. A. Halang, "Power electronics converters: Past, present and future," *Renew. Sustain. Energy Rev.*, vol. 81, no. 2, pp. 2028–2044, Jan. 2018.
[10] D. Jovcic and N. Strachan, "Offshore wind farm with centralised power conversion and DC interconnection," *IET Gener., Transmiss. Distrib.*, vol. 3, no. 6, pp. 586–595, Jun. 2009.
[11] T. D. Vrionis, X. I. Koutiva, N. A. Vovos, and G. B. Giannakopoulos, "Control of an HVDC link connecting a wind farm to the grid for fault ride-through enhancement," *IEEE Trans. Power Syst.*, vol. 22, no. 4, pp. 2039–2047, Nov. 2007.
[12] O. Gomis-Bellmunt, A. Junyent-Ferre, A. Sumper, and J. Bergas-Jane, "Control of a wind farm based on synchronous generators with a central HVDC-VSC converter," *IEEE Trans. Power Syst.*, vol. 26, no. 3, pp. 1632–1640, Aug. 2011.
[13] Z. Lubosny, *Wind Turbine Operation in Electric Power Systems*. Berlin, Germany: Springer, 2003.
[14] F. D. Bianchi, H. D. Battista, and R. J. Mantz, *Wind Turbine Control Systems*. Berlin, Germany: Springer, 2007.
[15] A. Meng, Z. Li, H. Yin, S. Chen, and Z. Guo, "Accelerating particle swarm optimization using crisscross search," *Inf. Sci.*, vol. 329, pp. 52–72, Feb. 2016.
[16] P. Li, D. Xu, Z. Zhou, W.-J. Lee, and B. Zhao, "Stochastic optimal operation of microgrid based on chaotic binary particle swarm optimization," *IEEE Trans. Smart Grid*, vol. 7, no. 1, pp. 66–73, Jan. 2016.
[17] K. L. Lian, J. H. Jhang, and I. S. Tian, "A maximum power point tracking method based on perturb-and-observe combined with particle swarm optimization," *IEEE J. Photovolt.*, vol. 4, no. 2, pp. 626–633, Mar. 2014.
[18] R. B. A. Koad, A. F. Zobaa, and A. El-Shahat, "A novel MPPT algorithm based on particle swarm optimization for photovoltaic systems," *IEEE Trans. Sustain. Energy*, vol. 8, no. 2, pp. 468–476, Apr. 2017.
[19] R. Li, W. Wang, and M. Xia, "Cooperative planning of active distribution system with renewable energy sources and energy storage systems," *IEEE Access*, vol. 6, pp. 5916–5926, 2018.
[20] S. Pookpunt and W. Ongsakul, "Design of optimal wind farm configuration using a binary particle swarm optimization at Huasai district, Southern Thailand," *Energy Convers. Manage.*, vol. 108, pp. 160–180, Jan. 2016.
[21] I. Khan, Y. Xu, H. Sun, and V. Bhattacharjee, "Distributed optimal reactive power control of power systems," *IEEE Access*, vol. 6, pp. 7100–7111, 2018.
[22] J. G. Slootweg, S. W. H. D. Haan, H. Polinder, and W. L. Kling, "General model for representing variable speed wind turbines in power system dynamics simulations," *IEEE Trans. Power Syst.*, vol. 18, no. 1, pp. 144–151, Feb. 2003.
[23] S. Zergane, A. Smaili, and C. Masson, "Optimization of wind turbine placement in a wind farm using a new pseudo-random number generation method," *Renew. Energy*, vol. 125, pp. 166–171, Sep. 2018.

**SI-ZHE CHEN** was born in Shantou, Guangdong, China, in 1981. He received the B.Sc. degree in mechatronics engineering and the Ph.D. degree in control theory and control engineering from the South China University of Technology, Guangzhou, China, in 2005 and 2010, respectively. He is currently an Associate Professor with the School of Automation, Guangdong University of Technology, Guangzhou. His general research interests include the control and power electronics technology in renewable energy.

**GUOZHUAN XIONG** was born in Jiujiang, Jiangxi, China, in 1992. He received the B.Sc. degree in automation from Jiujiang University, Jiujiang, in 2015. He is currently pursuing the the M.Sc. degree in control science and engineering from the School of Automation, Guangdong University of Technology, Guangzhou, China. His current research interest is mainly wind power generation control technology.

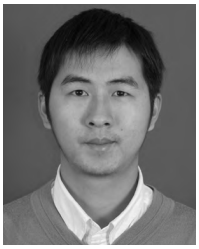

**GUIDONG ZHANG** (M'13) was born in Shantou, Guangdong, China, in 1986. He received the B.Sc. degree from the Xi'an University of Technology in 2008, the Ph.D. degree from the South China University of Technology in 2014, and the Ph.D. degree from the University of Hagen in 2015. He is currently an Associate Professor with the School of Automation, Guangdong University of Technology, Guangzhou. His research interests include power electronics topology and their applications.

**SAMSON SHENGLONG YU** (S'15) received the master's degree (Hons.) in electrical and electronic engineering and the Ph.D. degree in electrical power engineering from The University of Western Australia, Perth, Australia, in 2014 and 2017, respectively, where he is currently a Post-Doctoral Research Associate. His research interests include renewable energy integration and forecasting, power system analysis and control, smart grids, microgrid modeling, demand response, and dynamic state estimation. He received the first and second prizes in the IEEE Australia Council Paper Contest in 2015 and 2016.

**HERBERT HO-CHING IU** (S'98–M'00–SM'06) received the B.Eng. degree (Hons.) in electrical and electronic engineering from The University of Hong Kong, Hong Kong, in 1997, and the Ph.D. degree in electronic and information engineering from The Hong Kong Polytechnic University, Hong Kong, in 2000.

In 2002, he joined the School of Electrical, Electronic and Computer Engineering, The University of Western Australia, where he is currently a Professor. His research interests include power electronics, renewable energy, nonlinear dynamics, current sensing techniques, and memristive systems.

Dr. Iu currently serves as an Associate Editor for the IEEE TRANSACTIONS ON POWER ELECTRONICS, the IEEE TRANSACTIONS ON SMART GRIDS, the IEEE TRANSACTIONS ON NETWORK SCIENCE AND ENGINEERING, the IEEE TRANSACTIONS ON CIRCUITS AND SYSTEMS–II, and the IEEE ACCESS.

**TYRONE FERNANDO** (M'95–SM'05) received the B.E. (Hons.) and Ph.D. degrees from the University of Melbourne in Engineering, in 1990 and 1996, respectively.

In 1996, he joined the School of Electrical Electronic and Computer Engineering, The University of Western Australia, where he is currently a Professor. His research interests are power systems, renewable energy, state estimation, and biomedical engineering.

Dr. Fernando has served as an Associate Editor for the IEEE TRANSACTIONS ON INFORMATION TECHNOLOGY IN BIOMEDICINE and also a Guest Editor for the *Journal of Optimal Control Applications and Methods.* He is currently an Associate Editor of the IEEE TRANSACTIONS ON CIRCUITS AND SYSTEMS–II and the IEEE ACCESS.

**YUN ZHANG** received the B.Sc. and M.Sc. degrees in automatic engineering from Hunan University, Changsha, China, in 1982 and 1986, respectively, and the Ph.D. degree in automatic engineering from the South China University of Technology, Guangzhou, China, in 1998.

He is currently a Professor with the School of Automation, Guangdong University of Technology, Guangzhou. His current research interests include intelligent control systems, network systems, and signal processing.